Limit Cycle Oscillation amplitude tailoring based on Describing Functions and μ Analysis

Andrea Iannelli, Andrés Marcos, Mark Lowenberg

Abstract Freeplay is a nonlinearity commonly encountered in aeroservoelastic applications which is known to cause Limit Cycle Oscillations (LCOs), limited amplitude flutter phenomena not captured by a linear analysis. Uncertainties in the models are also known to play an important role in triggering instabilities which might not be present in the nominal case, or altering their features in an unpredictable way. This paper shows the process to build a framework to study the nonlinear behavior of a typical section affected by a freeplay in the control surface and uncertainties in its parameters' values. Starting from the definition of the nominal aeroelastic model, the nonlinear framework is implemented by means of the Describing Function (DF) method and robust analysis is introduced by means of μ technique. In addition, it is shown an idea to perform a tailoring of the LCO graph of the system with the practical goal to limit the oscillation amplitude. Implications and advantages of using DF and μ as primary tools are highlighted, and prowess of the methodology is showcased with an example.

1 Introduction

One of the major challenges faced by aeronautical industry nowadays is to achieve lightweight aircraft configurations which enable to reduce fuel consumptions and operating costs ensuring at the same time a feasible design in terms of safety constraints. Among the most dangerous instability phenomena exacerbated by wing flexibility there is flutter.

Flutter is a self-excited instability in which aerodynamic forces acting on a flexible body couple with its natural structural vibration modes producing oscillatory motion. The level of vibration may result in sufficiently large amplitudes to provoke

---

Andrea Iannelli, Andrés Marcos, Mark Lowenberg
Department of Aerospace Engineering, University of Bristol, BS8 1TR, United Kingdom, e-mail: andrea.iannelli/andres.marcos/m.lowenberg@bristol.ac.uk

failure and often this requirement dictates the design of the structure. The study of this problem hence entails a multi-disciplinary approach, involving structural dynamics and aerodynamics, commonly tackled by means of aeroelasticity. Flutter analysis has been widely investigated and several well-established techniques are available, representing the state-of-practice (see [11] for a thorough review).

Despite the large amount of effort spent in understanding flutter, it is acknowledged that predictions based only on computational analyses are not totally reliable. Currently this is compensated by the addition of conservative safety margins to the analysis results as well as expensive flutter test campaigns. One of the main criticalities arises from the sensitivity of aeroelastic instability to small variations in parameter and modeling assumptions. In addressing this issue, in the last two decades researchers looked at robust modeling and analysis techniques from the robust control community, specifically linear fractional transformation (LFT) models and μ (structured singular value) analysis [19, 25]. The so-called flutter robust analysis [17, 5] aims to quantify the gap between the prediction of the nominal stability analysis (model without uncertainties) and the worst-case scenario when the whole set of uncertainties is contemplated. In recent studies [12, 13, 16] other issues of this consolidated framework have been considered as: better understanding of the modelling options and their effects on the predictions, application of μ as flutter sensitivity tool and reconciliation of the robust analyses results with the physical understanding of the systems.

The framework of μ technique is straightforwardly applicable to the study of robust stability (RS) and performance (RP) of linear plants. However the increase in flexibility on one side and a more realistic description of the system on the other compel to consider cases where the linear hypothesis no longer holds. Aeronautical industry, for example, has recently shown interest in evaluating the effect of the uncertainties on instabilities prompted by the control surface freeplay [20].
A way to introduce nonlinearities in the frequency domain framework, borrowed from the control community, is represented by the Describing Function (DF) method [9]. This has been employed for the prediction of onset, frequency and amplitude of Limit Cycle Oscillations (LCOs) in aeroservoelastic applications [10, 7].

The present study applies the framework μ-DF to a well-known benchmark [22] in order to assess the nonlinear flutter behavior of a typical section configuration with control surface freeplay. Within the showcased framework, μ analysis can be applied in order to investigate the robustness of the LCO in the face of uncertainties [3]. Here a novel application of these tools to the study of nonlinear systems is proposed, which enables to exploit the worst-case capability of μ in order to tailor the LCO properties of the system with the smallest effort in terms of change of nominal design (*optimal passive* design remedies).

The layout of the article is as follows. Sect. 2 presents the linear system considered in the analyses. An overview for each one of the techniques employed in the work (DF, LFT and μ) is given in Sect. 3. In Sect. 4 the application of the built framework to the chosen test bed is shown. The rationale behind the proposed tailoring of the nonlinear behavior of the system and the corresponding results are provided in Sect. 5. Finally, Sect. 6 gathers the main conclusions of the work.

2 Typical Section system

2.1 Model

The *typical section* model was introduced in the early stages of aeroelasticity to investigate dynamic phenomena such as flutter [4]. Despite its simplicity, it captures essential effects in a simple model representation, see Fig. 1.

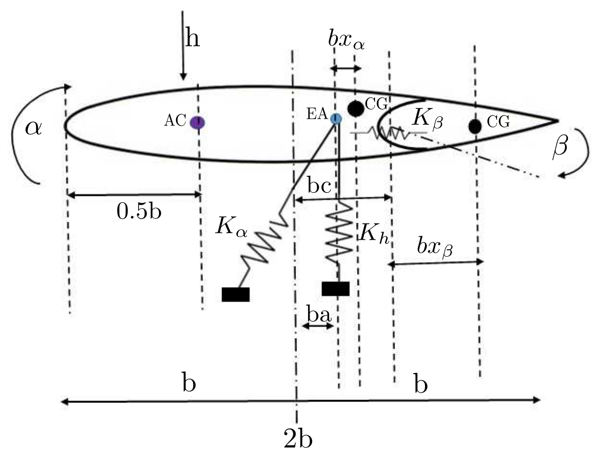

Fig. 1 Typical section sketch

From the structural side, it basically consists of a rigid airfoil with lumped springs simulating the 3 degrees of freedom of the section: plunge h, pitch α and trailing edge flap β. The positions of the elastic axis (EA), center of gravity (CG) and the aerodynamic center (AC) are also marked. The main parameters in the model, see Fig. 1, are: K_h, K_α and K_β –respectively the bending, torsional and control surface stiffness; half chord distance b; dimensionless distances a, c from the mid-chord to respectively the flexural axis and the hinge location, and x_α and x_β, which are dimensionless distances from flexural axis to airfoil center of gravity and from hinge location to control surface center of gravity. S_α and S_β, not explicitly reported in the picture and employed later on in the analyses, are the equivalent of the latter with dimension, i.e. $S_\alpha = bx_\alpha$ and $S_\beta = bx_\beta$.
In addition to the above parameters, the inertial characteristics of the system are given by: the wing mass per unit span m_s, the moment of inertia of the section about the elastic axis I_α, the moment of inertia of the control surface about the hinge I_β. If structural damping is considered, this can be expressed specifying the damping ratios for each DOFs and then applied through modal damping approach [6].

The Theodorsen unsteady formulation proposed in [23] is employed as aerodynamic model. This approach is based on the assumption of a thin airfoil moving with small harmonic oscillations in a potential and incompressible flow. Despite its simplicity, such idealization is pertinent to flutter analysis since this implies a condition of neutral stability of the system. The same hypotheses underline most of more improved aerodynamic approaches (e.g. Doublet Lattice Method).

In order to present the basic model development approach, $\mathbf{X}$ and $\mathbf{L_a}$ are defined as the vectors of the degrees of freedom and of the aerodynamic loads respectively:

$$\mathbf{X}(t) = \begin{bmatrix} \frac{h(t)}{b} \\ \alpha(t) \\ \beta(t) \end{bmatrix}; \quad \mathbf{L_a}(t) = \begin{bmatrix} -L(t) \\ M_\alpha(t) \\ M_\beta(t) \end{bmatrix} \tag{1}$$

The set of differential equations describing the dynamic equilibrium [11] can then be recast in matrix form using Lagrange's equations:

$$\left[\mathbf{M_s}\right]\ddot{\mathbf{X}} + \left[\mathbf{C_s}\right]\dot{\mathbf{X}} + \left[\mathbf{K_s}\right]\mathbf{X} = \mathbf{L_a} \tag{2}$$

where $\left[\mathbf{M_s}\right]$, $\left[\mathbf{C_s}\right]$ and $\left[\mathbf{K_s}\right]$ are respectively the structural mass, damping and stiffness matrices. The expression of $\mathbf{L_a}$, provided in the Laplace s domain, is:

$$\begin{aligned} &\mathbf{L_a}(s) = q\left[\mathbf{A}(\bar{s})\right]\mathbf{X}(s) \\ \text{with} \quad &\mathbf{L_a}(s) = \mathscr{L}\left[\mathbf{L_a}(t)\right]; \quad \mathbf{X}(s) = \mathscr{L}\left[\mathbf{X}(t)\right] \end{aligned} \tag{3}$$

where the dynamic pressure q and the dimensionless Laplace variable $\bar{s}$ (=$s\frac{b}{V}$ with V the airspeed) are introduced. $\mathbf{A}(\bar{s})$ is called the generalized Aerodynamic Influence Coefficient (AIC) matrix, and is composed of generic terms $\mathbf{A}(\bar{s})_{ij}$ representing the transfer function from each degree of freedom j in $\mathbf{X}(s)$ to each aerodynamic load component i in $\mathbf{L_a}(s)$.
Due to the expression of the AIC matrix which does not have a rational dependence on the Laplace variable s, the final aeroelastic equilibrium is inherently expressed in frequency-domain and is given by:

$$\left[\left[\mathbf{M_s}\right]s^2 + \left[\mathbf{C_s}\right]s + \left[\mathbf{K_s}\right]\right]\mathbf{X} = q\left[\mathbf{A}(\bar{s})\right]\mathbf{X} \tag{4}$$

A rational approximation of $\left[\mathbf{A}(\bar{s})\right]$ has to be performed in order to express the equilibrium in state space, which is essential to deal with aeroservoelastic problems and control based techniques. In this work Minimum State (MS) [14] method is employed, which propose the following expression for the aerodynamic operator:

$$\left[\mathbf{A}\right] \approx \left[\mathbf{A}_{MS}\right] = \left[\mathbf{A_2}\right]\bar{s}^2 + \left[\mathbf{A_1}\right]\bar{s} + \left[\mathbf{A_0}\right] + \left[\mathbf{D}'\right]\left(\bar{s}\left[\mathbf{I}\right] - \left[\boldsymbol{\Gamma}\right]\right)^{-1}\left[\mathbf{E}'\right]\bar{s} \tag{5}$$

Where $\left[\mathbf{A_i}\right]$ are real coefficient matrices obtained imposing a matching of the operators ($\mathbf{A}$ and $\mathbf{A}_{MS}$) at determined frequencies of oscillations. The last block consists of the so-called *lag terms* which basically represent high-pass filters of the form $\frac{\bar{s}}{\bar{s}+\gamma_i}$ with the aerodynamic roots γ_i as cross-over frequencies (defining the diagonal matrix $\boldsymbol{\Gamma}$) and the gains provided by the real matrices $[\mathbf{D}']$ and $[\mathbf{E}']$. They are iteratively determined through a nonlinear least square since Eq.(5) is bilinear in these two unknowns. The impact on robust flutter analysis of the different expressions for the AIC matrix (original frequency-domain operator or state-space approximations) when aerodynamic uncertainties are considered has been investigated in [12].

The resulting state-space equation, which includes N augmented aerodynamic states equal in number to the lag roots γ_i, is here reported in short-hand notation:

$$\begin{bmatrix} \dot{\hat{\mathbf{X}}}_\mathbf{s} \\ \dot{\hat{\mathbf{X}}}_\mathbf{a} \end{bmatrix} = \begin{bmatrix} \chi_{ss} & \chi_{sa} \\ \chi_{as} & \chi_{aa} \end{bmatrix} \begin{bmatrix} \hat{\mathbf{X}}_\mathbf{s} \\ \hat{\mathbf{X}}_\mathbf{a} \end{bmatrix} \tag{6}$$

Where $\hat{\mathbf{X}}_\mathbf{s}$ and $\hat{\mathbf{X}}_\mathbf{a}$ are respectively the vector of structural and aerodynamic states.

2.2 Linear Nominal Flutter Analysis

Nominal flutter analysis studies the conditions at which the dynamic aeroelastic system loses its stability. As the airspeed V varies the system's behavior in terms of response and stability changes. The result is the prediction of the so-called flutter speed V_f, below which the system is guaranteed to be stable.

The stability of the system studied here is related to the spectrum of the state-matrix defined in Eq.(6). Six aerodynamic roots γ_i equally spaced between 0.1 and 0.7 are chosen to approximate the Theodorsen operator. This is done in order to span the range of reduced frequencies where the flutter frequency is expected to be.

The nominal parameters defining the typical section studied in this work are taken from [22]. This test bed focuses on a three degrees of freedom typical section configuration with control surface freeplay. This nonlinearity, which will be examined later in Sect. 3.1.2, affects the diagonal term of the matrix $\mathbf{K_s}$ corresponding to the control surface rotation (i.e. K_β). If this term is assumed as K_β^L (i.e. the control surface stiffness without freeplay) and all the other parameters hold their nominal values, a linear analysis of the system can be performed.

In Fig. 2 the eigenvalues corresponding to the structural modes of the system are depicted as the airspeed increases from 1 $\frac{m}{s}$ (square marker) to 30 $\frac{m}{s}$. The system exhibits a plunge-pitch flutter, highlighted with the circle marker. This phenomenon is commonly called *binary flutter* since it is mainly featured by the interaction of two modes.
In Tab.1 a comparison for the linear flutter speed V_L with the ones reported in other works studying this problem is reported.

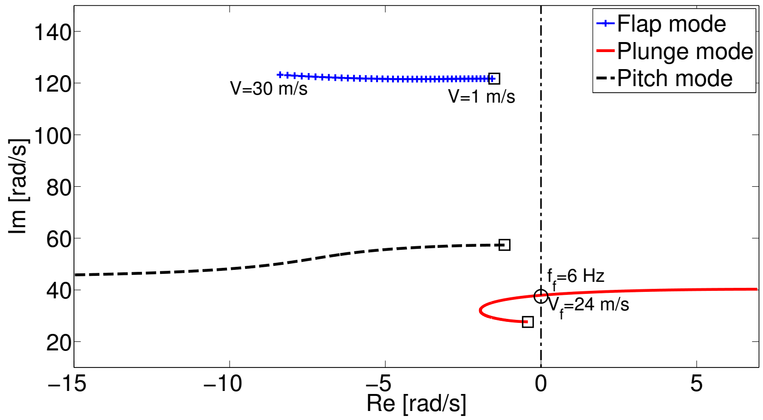

Fig. 2 Nominal linear system: pole locations as a function of airspeed

Table 1 Comparison of results in terms of flutter speed and frequency for the linear case

	Flutter velocity [$\frac{m}{s}$]	Flutter frequency [Hz]
Present work	24	6
[18]	23.9	6.1
[6]	23.9	6
[3]	23.2	6

3 Quasi-linear robust framework

3.1 Describing Function Method

The analysis and design of linear control plants pivots on a complex-valued function, the frequency response. However, this function cannot be defined for nonlinear systems, hence frequency domain techniques cannot be directly applied. The Describing Function (DF) method [9, 15] aims to overcome this obstacle by providing in these cases an alternative definition of frequency response. The basic concepts of this technique are here presented, with particular emphasis on this application.

3.1.1 Main concept

The concept of *quasi-linearization* is the basis of the application of DF. This expedient originates by the goal to retain the advantages of a linear approximation without the constraint of requiring small departures of the variables from the nominal operating values. This can be achieved if the approximation of the nonlinear operator depends on some properties of the input. Dependence of performance on signal amplitude, the basic characteristic of nonlinear behavior, is thus retained.

The DF method is mostly applied to systems which can be recast in the framework of Fig. 3. This class of system is characterised by having separable linear and nonlinear parts connected in a single loop configuration, which is often the case in the field of aeroservoelasticity [8] (e.g saturation, freeplay, hysteresis).

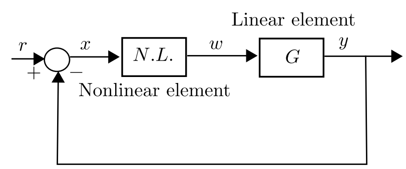

Fig. 3 Feedback representation of a nonlinear system

The quasi-linearization process requires that the input signal *form* is specified. In analogy to what is done in frequency domain analysis, it is widely employed the concept of sinusoidal-input describing function (SIDF), in the following simply abbreviated as DF. The interest in periodic signals is mainly dictated by the aim to detect and analyse steady oscillations in nonlinear systems, also known as Limit Cycle Oscillations (LCOs).
The *key* hypothesis of the DF method is that only the fundamental component has to be retained from the generical periodic output w(t). This is an approximation because the output of a nonlinear element corresponding to a sinusoidal input usually contains higher harmonics. This is motivated by the assumption that the higher harmonics in the output are filtered out, i.e. the linear element satisfies the low-pass filter condition (or *filter hypothesis*):

$$\|G(j\omega)\| \gg \|G(jn\omega)\| \quad \text{for} \quad n = 2, 3, \ldots \tag{7}$$

The DF of a nonlinear element is thus the complex fundamental-harmonic gain of a nonlinearity in the presence of a driving sinusoid of amplitude A:

$$\begin{aligned} &N(A,\omega) = \frac{Me^{j(\omega t+\phi)}}{Ae^{j(\omega t)}} = \frac{M}{A}e^{j\phi} = \frac{b_1 + ja_1}{A} \\ \text{with} \quad &x = A\sin(\omega t); \quad w(t) \approx a_1(A,\omega)\cos(\omega t) + b_1(A,\omega)\sin(\omega t) \\ &M(A,\omega) = \sqrt{a_1^2 + b_1^2}; \quad \phi(A,\omega) = \arctan(\frac{a_1}{b_1}) \end{aligned} \tag{8}$$

This method hence consists in treating the nonlinear element of Fig. 3 in the presence of sinusoidal input as if it were a linear element with a frequency response $N(A,\omega)$.

3.1.2 DF for the freeplay nonlinearity

Due to the well established usage of DF method in control community, the expression of $N(A,\omega)$ can be found for the majority of nonlinearities commonly encountered in applications [9]. Freeplay, also called dead-zone or threshold, often arises in mechanical and electrical systems where the first part of the input is needed to overcome an initial opposition at the output, as schematically depicted in Fig. 4(a). Its explicit mathematical definition (refer to Fig. 4(a) for the symbology) is given by:

$$w = \begin{cases} k(x-\delta); & |x| > \delta \\ 0; & |x| < \delta \end{cases} \tag{9}$$

Having defined the (positive) freeplay size δ, the describing function N^F, obtained analytically, is then:

$$N^F(A) = \begin{cases} 0; & A < \delta \\ \frac{k}{\pi}\left[\pi - 2\sin^{-1}(\frac{\delta}{A}) - 2(\frac{\delta}{A})\sqrt{1-(\frac{\delta}{A})^2}\right]; & A > \delta \end{cases} \tag{10}$$

Due to the properties (static and memoryless) hold by this nonlinearity, its describing function is a pure real gain not depending on frequency, but only on the amplitude A of the signal, in particular on its ratio with δ. In Fig. 4(b) N^F is depicted for the case k=1.

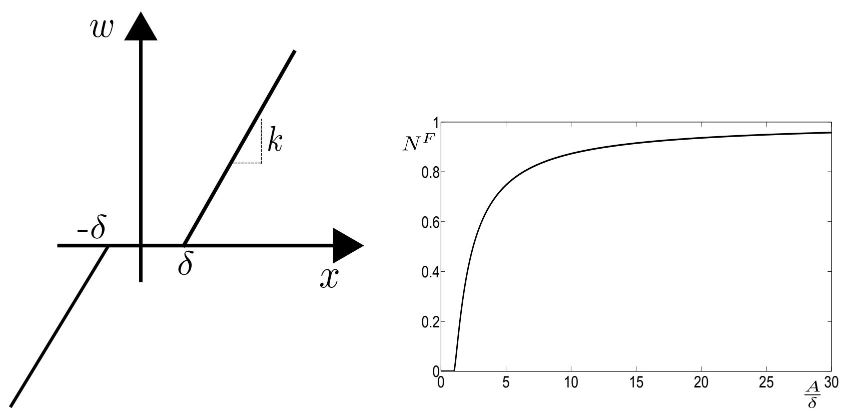

(a) Freeplay nonlinearity (b) Associated Describing Function

Fig. 4 Freeplay nonlinearity: graphical representation and associated Describing Function

3.1.3 Detection of LCOs

One of the main applications of DF method is the study of the existence of steady oscillations in a nonlinear system. In particular Limit Cycle Oscillations (LCOs) [24] are of engineering interest, which are defined as initial condition-independent isolated periodic orbits which occurs in unforced dissipative systems. LCOs are usually avoided in mechanical systems since they are likely to reduce fatigue's life and provoke critical damages. The aeronautical industry has sensibly strengthen his focus on this phenomena in the last decade [8] and thus increasing effort has been devoted on this topic by the research community. It is well ascertained that the knowledge of the existence of a limit cycle, as well as its approximate amplitude and frequency, is a prerequisite for a good system design [20].
The methodology employed to study LCOs through DF takes the clue from the feedback representation of a nonlinear system in Fig. 3, specialised in Fig. 5 by specifying the signal circulating through the system as a sinusoid, thus replacing the nonlinear element by its describing function N, and considering null input (since focus is on stability properties of the system).

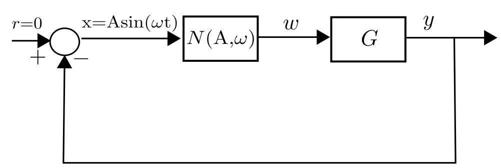

Fig. 5 Quasi-linearized system specialised for LCOs study through DF

Linear theory is then applied to the quasi-linearized system, searching for points of neutral stability which are interpreted as LCOs in the original (nonlinear) system. The well-known feedback relations involve the frequency response of the signals (in capital letters) and the transfer functions of the operators, and the resulting necessary condition for oscillations are:

$$\begin{aligned} &X(j\omega) = -G(j\omega)W(j\omega) \\ &W(j\omega) = N(j\omega)X(j\omega) \\ &\left[1 + G(j\omega)N(A,\omega)\right]X(j\omega) = 0 \end{aligned} \tag{11}$$

Solution of the characteristic equation gives the conditions in terms of A and ω such that the system exhibits self-sustained oscillations.

The characteristic equation in Eq.(11) gives only a necessary condition for the occurrence of periodic oscillations in the nonlinear system. Indeed stability of the oscillation has still to be verified. The question of LCO stability is generally posed in terms of the states trajectory behavior following amplitude or frequency perturbations. If the LCO returns to its original equilibrium state it is defined *stable*, otherwise it is *unstable*. To tackle the stability problem, the methodology proposed in [2] is here adopted. The idea is to study the variation of the real part σ of the eigenvalue associated to the LCO solution following a perturbation in A. A stable limit cycle requires $\frac{\partial\sigma}{\partial A} < 0$, since a positive perturbation in amplitude moves the trajectory outside the limit cycle and requires a decay in the amplitude (negative real part) to move the trajectory back to the limit cycle, and conversely an unstable limit cycle will have $\frac{\partial\sigma}{\partial A} > 0$.

3.2 Linear Fractional Transformation and μ analysis

Robust flutter analysis [17] deals with flutter instability predictions when the aeroelastic model is subject to uncertainties. Examples of the latter are low confidence in the values of parameters and coefficients of the matrices, or neglected dynamics in the nominal model. Once the problem is described within the LFT framework, μ analysis enables to predict for a given airspeed if the set of uncertainties is capable to lead to instability. A very brief description of these tools is here provided (see [19, 25] and references herein).

If the *coefficient matrix* $\mathbf{M}$ is defined as a proper transfer matrix, $\mathscr{F}_u$, namely the upper LFT, is the closed-loop transfer matrix from input $\mathbf{u}$ to output $\mathbf{y}$ when the nominal plant $\mathbf{M_{22}}$ is subject to a perturbation matrix $\boldsymbol{\Delta_u}$ (Fig. 6).

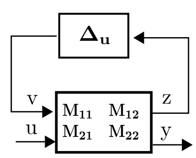

$$\mathbf{v} = \mathbf{\Delta_u z}$$
$$\mathbf{z} = \mathbf{M_{11}v} + \mathbf{M_{12}u}$$
$$\mathbf{y} = \mathbf{M_{21}v} + \mathbf{M_{22}u}$$

Fig. 6 Upper LFT

$\mathbf{M_{11}}$,$\mathbf{M_{12}}$ and $\mathbf{M_{21}}$ reflect a priori knowledge of how the perturbation affects the nominal map. Once all varying or uncertain parameters are *pulled out* of the nominal plant, the problem appears as a nominal system subject to an artificial feedback. The algebraic expression for $\mathscr{F}_u$ is given by:

$$\mathscr{F}_u(\mathbf{M}, \boldsymbol{\Delta_u}) = \mathbf{M_{22}} + \mathbf{M_{21}}\boldsymbol{\Delta_u}(\mathbf{I} - \mathbf{M_{11}}\boldsymbol{\Delta_u})^{-1}\mathbf{M_{12}} \tag{12}$$

This LFT is well posed if and only if the inverse of $(\mathbf{I} - \mathbf{M_{11}}\boldsymbol{\Delta_u})$ exists.

The structured singular value $\mu_{\boldsymbol{\Delta}}(\mathbf{M})$ of a matrix $\mathbf{M} \in C^{n\times n}$ with respect to the uncertain matrix $\boldsymbol{\Delta}$ is defined below:

$$\mu_{\boldsymbol{\Delta}}(\mathbf{M}) = \frac{1}{\min_{\boldsymbol{\Delta}}(\bar{\sigma}(\boldsymbol{\Delta}) : \det(\mathbf{I} - \mathbf{M}\boldsymbol{\Delta}) = 0)} \tag{13}$$

where $\bar{\sigma}(\boldsymbol{\Delta})$ is the maximum singular value of $\boldsymbol{\Delta}$ and $\mu_{\boldsymbol{\Delta}}(\mathbf{M}) = 0$ if there is no $\boldsymbol{\Delta}$ satisfying the determinant condition. Note that this definition can be specialized to determine whether the LFT $\mathscr{F}_u(\mathbf{M},\boldsymbol{\Delta_u})$ is well posed once the generic matrix $\mathbf{M}$ in the above definition is replaced by $\mathbf{M_{11}}$ and $\boldsymbol{\Delta}$ belongs to the corresponding uncertainty set $\boldsymbol{\Delta_u}$. For ease of calculation and interpretation, this set is typically norm-bounded $\|\boldsymbol{\Delta}\|_\infty < 1$ (without loss of generality by scaling of $\mathbf{M_{11}}$). In this manner, if $\mu_{\boldsymbol{\Delta}}(\mathbf{M_{11}}) \leq 1$ then the result guarantees that the analyzed system is robustly stable (RS) to the considered uncertainty.

4 Analysis of the Typical Section LCO due to freeplay

Considerable work has been done in the past two decades in investigating the effects of structural nonlinearities on aeroelastic phenomena. Examples of this effort are the experimental [6] and analytical studies [22] conducted to precisely assess the nonlinear flutter behavior of a three-degrees-of-freedom typical section configuration with control surface freeplay. The analytical studies employed both the direct time integration and the DF method with the aim to determine LCO amplitudes and frequencies and offer a comparison of the predicted responses with experimental data. These benchmark results have driven further studies widening the investigations of this testcase: harmonic-balance [18], continuation methods [10] and μ analysis [3].

4.1 Detection of freeplay-induced LCOs

The investigations builds on the linear model described in Sect. 2.1 and the DF method to deal with the freeplay nonlinearity. The application of the latter enables to give an expression for the elastic moment M_β^E acted by the control surface:

$$
\begin{aligned}
M_\beta^E &= K_\beta^{QL}\beta \\
K_\beta^{QL} &= N^F(\beta)K_\beta^L
\end{aligned}
\tag{14}
$$

where K_β^L is the flap stiffness in the linear case (δ=0), K_β^{QL} is the quasi-linear flap stiffness and N^F is the DF provided in Eq.(10) and depicted in Fig. 4(b), specialised to this case taking k=1 and A=β. In other words, the linear stiffness K_β^L is replaced by an equivalent stiffness K_β^{QL} in the diagonal term of $\mathbf{K_s}$ corresponding to the control surface, which is a function of the flap rotation β.

The procedure to detect necessary conditions for LCO in the plant can thus be initialized. A fundamental harmonic solution for the flap rotation β=$\beta_s\sin(\omega t)$ is assumed and from Eq.(10) the corresponding value of N^F is obtained (the freeplay size δ is fixed). This enables to calculate the quasi-linear stiffness K_β^{QL} from Eq.(14) and thus evaluate through eigenvalue analysis the corresponding flutter speed V_f, defined as the lowest airspeed which drives the system unstable, and the corresponding flutter frequency ω_f, as outlined in Sect.2.2 for a value of the stiffness corresponding to K_β^L. Due to the existing relation between K_β^{QL} and β_s, the results can then be shown using graphs K_β^{QL}-V_f and K_β^{QL}-ω_f if the focus is on linear flutter features, or analogously using V_f-β_s and V_f-ω_f if the LCO phenomenon is emphasized. As stressed later on, these two representations are directly related since they both originate from the procedure just described. The DF method is instrumental in guaranteeing the connection and enabling to transfer the information coming from multiple linear flutter analyses to LCO characterization.

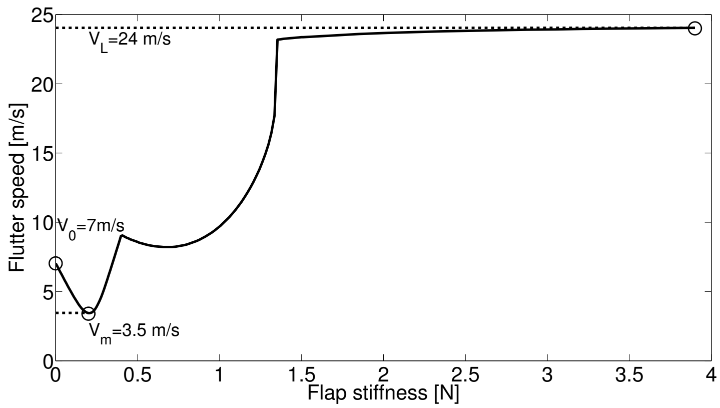

(a) Flutter speed versus flap stiffness

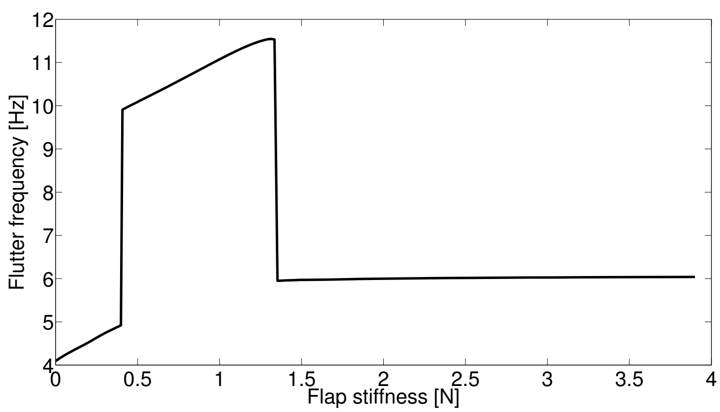

(b) Flutter frequency versus flap stiffness

Fig. 7 Flutter speed and frequency vs flap stiffness as $K_\beta^{QL} \in [0, K_\beta^L]$

Figure 7(a) shows the values of flutter speed corresponding to a variation of the flap stiffness between 0 and the linear value K_β^L (that is, as the associated describing function N^F varies from 0 and 1). Important airspeeds are highlighted: V_0 is the flutter speed for zero stiffness of the control surface; V_m is the minimum flutter

speed, attained for $K_\beta^{QL} \approx 0.2$ N; V_L is the linear flutter speed (determined in Fig. 2). Fig. 7(b) shows the values of the flutter frequencies.
It is worth noticing, recalling Fig. 7(b), that two distinctive flutter frequencies are detected, as the value of the flap stiffness is varied. This aspect is important for what will be considered in Sect.5, thus it is here further investigated.
In Fig. 8 it is shown a plot similar to the one reported in Fig. 7(a), but in this case considering *all* the airspeeds which correspond to a crossing of the imaginary axis, and not only the lowest (i.e. V_f). It is apparent from the graph that for a large range of flap stiffness (0 N< K_β^{QL} <1.3 N) both pitch and plunge modes experience instability. In particular, three regions can be clearly detected: in the first one, characterized by $K_\beta^{QL} \in [0, 0.4]$ N, the plunge mode is the first to go unstable (flutter frequency $\approx$ 4-5 Hz); in the second region, $K_\beta^{QL} \in [0.4, 1.3]$ N, the pitch mode is responsible for the lowest unstable speed (flutter frequency $\approx$ 10-11 Hz); finally, for
$K_\beta^{QL} \in [1.3\ \mathrm{N}, K_\beta^L]$, only the plunge mode goes unstable (flutter frequency = 6 Hz). The unstable eigenvalue is associated to its elastic mode through the application of the Modal Assurance Criteria [1]. The abrupt jumps in Fig. 7(b) has thus to be ascribed to the change in the elastic mode reaching earlier the flutter condition, which depends on the value of flap stiffness.

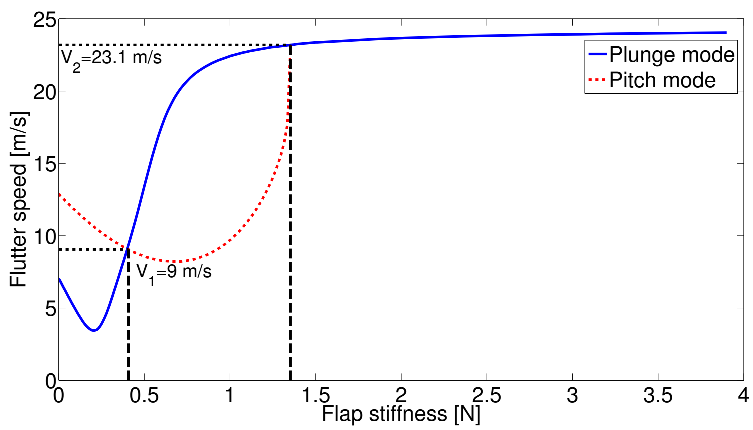

Fig. 8 Flutter speed vs flap stiffness associated at each elastic mode by means of MAC

Based on the previous analyses, the DF method enables to infer conclusions about the nonlinear response of the system due to the freeplay, i.e. amplitude, frequency and stability of LCOs. In particular, the conditions of neutral stability for the quasi-linearized system (reported in Fig. 7(a)) are associated to LCOs of the nonlinear system, with amplitude obtained from Eq.(14) and frequency provided by Fig. 7(b). In Fig. 9 the nondimensional flap rotation amplitude $\frac{\beta_s}{\delta}$ is plotted against the airspeed. Stable and unstable oscillations are depicted respectively with a continuous and dashed lines.

The shown results are in good agreement with what reported in the aforementioned references applying DF method to the same test case. The applicability of the filter hypothesis (Eq.7) is thoroughly addressed in [18]. In this work the Harmonic Balance, a refinement of DF method where also higher harmonics than the fundamental one can be retained, is employed. Two cases are studied, with respectively 1 harmonic, leading to equivalent results to the DF method, and 3 harmonics considered. In the latter case, the predictions almost perfectly match the results obtained through nonlinear time-marching, which is taken as the reference result. When only the first harmonic is considered, some discrepancy can be detected in the LCO branch of Fig. 9 corresponding to the low frequency instability, with a higher amplitude predicted. It is also observed that test data [6], especially in terms of oscillation amplitude, are for some small airspeed ranges only approximately captured. This is ascribed in [10] to more complex limit cycles that exhibit several types of nonlinear behavior including quasiperiodicity and thus can not be correctly modelled in this framework. It is however concluded by many [6, 10, 22, 3] that DF represents a valid tool of analysis for this problem.

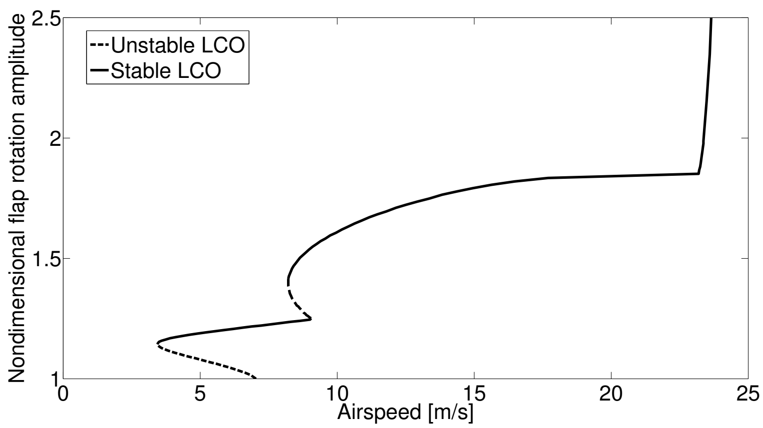

Fig. 9 Flap rotation LCO amplitude $\frac{\beta_s}{\delta}$ against airspeed. Stable and unstable oscillations highlighted

5 LCO graph Tailoring

In [3] it is tackled the task to provide robust stability assessment of this benchmark problem by means of μ analysis. The chief goal is to quantitatively evaluate the degradation of the curve in Fig. 9 in terms of amplitude increase and change in critical airspeeds. Each point of the plot corresponds to a quasi-linearization of the system, and thus can be recast in the LFT framework (Eq.12) and its stability analysed by means of μ. In this section a different perspective on the LCO study adopting robust techniques is proposed.

As an introduction, it is recalled that flutter is generally associated to catastrophic phenomena featured by oscillations with increasing amplitudes. The presence of nonlinearities tend to bound the amplitude of vibration, leading to limited amplitude flutter, generally named LCOs. These periodic oscillations, albeit less critical than a diverging response, can result in structural fatigue issues which might lead to failure, and in general undesired behavior of the airframe. There are no precise guidelines defining values of acceptable LCOs. While the overall goal is to limit the LCO amplitudes below the amplitudes caused due to turbulence during flight (and this poses a first requirement), one of the accepted industrial practices is to limit the resulting accelerations in prescribed points of the airframe [20]. These values can be related as well to the LCO amplitude. It hence emerges on the one side, the interest in quantitatively evaluating this phenomenon (e.g. as done in Sect. 4 by means of DF approach) and on the other hand to limit it. This can be achieved either by changing the design (*passive* methods) or directly during flight by feedback control (*active* methods).

The chief goal of this section is to demonstrate how μ analysis can be applied to tackle the task of achieving a reduction in LCO amplitude. The classic LFT-μ framework outlined in Sect.3.2 and Eqs.(12)-(13) is applied. The idea is to consider the quantities held in $\boldsymbol{\Delta}$ as *tailoring variables*, that is $\boldsymbol{\Delta}$ is the variable space made of parameters which can be exploited in order to achieve a better nonlinear behavior, here defined as an LCO curve featuring smaller amplitudes.

5.1 Object definition through DF framework

Recalled here the connection between the two plots described in Fig. 7(a) and Fig. 9. Specifically, the top plot Fig. 7(a) represents a linear flutter analysis applied to the system as the flap stiffness is varied. This curve is used as a basis to build the graph in Fig. 9 depicting the LCO amplitude as a function of the airspeed by making use of the relation given by the DF method between the flap amplitude and the quasi-linear stiffness (Eqs. 10-14). It is thus straightforward that decreasing the LCO amplitude is equivalent to moving towards the left the curve in Fig. 7(a). Note also that the points lying on this curve are all featured by a condition of neutral stability (they all have one eigenvalue with zero real part).

The structured singular value is usually applied to predict a measure of the distance of a stable plant from the neutral stability condition. In this particular case, it is employed to obtain the same measure for an *unstable* plant, attributing to it the meaning of distance to regain neutral stability. This usage of μ has to be considered exceptional and, when employed, care should be put in interpreting the results. In this application, the outcome provided by μ is not used to infer conclusions on the robustness of the plant, but, as better explained later, to understand how and which parameters should be modified to achieve the specified goal. In Fig. 10 it is depicted a pictorial explanation of this concept.

The nominal plant (having one eigenvalue with positive real part) is identified by the square marker and is specified by the nominal parameters of the system, the definition of an airspeed V and a value for the quasi-linear flap stiffness K_β^{QL}. The peak value found with μ analysis gives therefore the lowest size of perturbation matrix which leads to a neutral stability condition. After the perturbation pointed out by μ is applied to the system's parameters, the plant marked with the circle loses the condition of neutral stability, which is *allocated* to the one with the square. This graphically also means that the dashed curve, as desired, has moved towards the left, and hence the associated LCO exhibits smaller amplitude.

An important feature of this strategy is that it allows to specify the desired reduction in LCO amplitude at a certain airspeed V by selecting the value of K_β^{QL} at which the neutral stability condition is allocated. Moreover, the worst-case scenario nature of μ analysis turns to have here a very practical consequence: the critical perturbation matrix $\boldsymbol{\Delta}^{cr}$ (associated to the lower bound analysis) represents the *smallest* effort in terms of change of nominal design, because it shows the combination of parameters leading to the required goal with the overall minimum perturbation size. For this reason it is here referred to as an *optimal passive* design remedy.

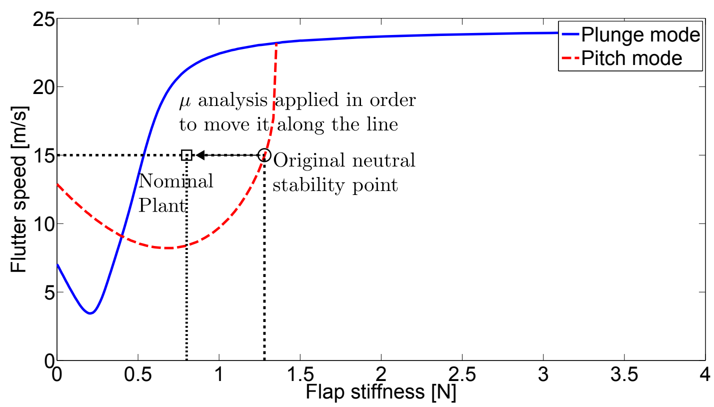

Fig. 10 Application of μ analysis to modify the LCO plot: definition of the nominal plant and depiction of the sought change in position of the neutral stability point

Fig. 10 recalls that there might be two different modes going unstable depending on the values of the flap stiffness. The selected plant for the analysis showed in the plot, for example, is *in between* the two instabilities. As a result, the combination of design parameters allowing a reduction in amplitude of the LCO associated to the pitch mode (dashed curve shifted left) could lead to an increase of the one associated to the plunge (continuous curve shifted right), with eventually only a partial or negligible objective achievement. Once defined the variable space, a μ-based sensitivity analysis as the one proposed in [13] is performed in order to detect which parameters affect more the pitch instability and less the plunge one and thus make effective and efficient design changes.

Finally, as a constraint on this tailoring, it is prescribed that the proposed improvement should not worsen the overall stability of the system, which can be characterized by means of the values of V_m and V_L (defined in Fig. 7(a)).

5.2 Application of μ for the LCO tailoring

This procedure starts with the definition of the nominal plant and the block $\boldsymbol{\Delta}$. The last task consists in the definition of the variable space for the tailoring. In the showcased example it includes terms of structural mass $\mathbf{M_s}$ and stiffness $\mathbf{K_s}$ matrices, but in principle no limitations exist for this choice. The following (each one with a range of variation of 20% from the nominal value) are selected: S_α, I_α, I_β, K_h and K_α. The LFT describing the problem is defined by the block:

$$\boldsymbol{\Delta}^{7,R} = \mathrm{diag}(\delta_{S_\alpha}\mathbf{I}_2, \delta_{I_\alpha}, \delta_{I_\beta}\mathbf{I}_2, \delta_{K_h}, \delta_{K_\alpha}) \qquad (15)$$

where the size of the uncertainties (total $\boldsymbol{\Delta}$ dimension) and their nature (R for real) is recalled in the superscripts. $\mathbf{I}_n$ indicates the identity matrix with size n (for repeated uncertainties). For what concerns the definition of the nominal plant, an airspeed is selected such that it lies in a region characterised by high LCO amplitude, for example V=15 $\frac{m}{s}$. Then a value of flap stiffness is chosen, which unequivocally defines the sought LCO amplitude for that operating point. A value of 0.85 N is taken, and hence the nominal plant corresponds to the one depicted with the square marker in Fig. 10.

The following step consists in performing the μ-based sensitivity analysis in order to understand which parameters among those in Eq.(15) affect the pitch instability responsible for the high amplitude branch, and how to modify those in order to achieve the goal. It is worth noticing that what is performed here consists basically in estimating the LCO amplitude sensitivity with respect to the parameters hold in $\boldsymbol{\Delta}$. In an active control perspective, this study could drive the design of the feedback control law to actively reduce the LCO amplitudes and possibly eliminate LCOs. The importance of this step is acknowledged in literature. In [21] for example this is tackled differentiating the equations based on the HB method and obtaining analytical sensitivities in the framework of the typical section. The method here adopted (not fully shown here due to space constraints) is believed to be less subject to the complexity of the plant analysed since it does not rely on analytical formulations, but it can be straightforwardly applied once the problem is recast in this framework. Based on the information provided by the sensitivity analysis, the following conclusions are inferred:

- The parameters that affect the pitch instability, but that do not affect the plunge one, can be advantageously taken as suggested by the worst-case analysis so as to achieve the objective, e.g. $\delta_{I_\alpha} = 1$ and $\delta_{I_\beta} = -1$
- The parameters that do not affect the pitch instability, but do affect the plunge one, can be taken with opposite sign to counteract potential undesired effect on it, e.g $\delta_{K_h} = -1$

- The parameters that affect in the same way the two instabilities (e.g. K_α) have to be carefully considered because of the multiple effects they may have.

With respect to the last point, it is worth remembering that this *optimization* process is subject to the constraint of preserving similar values for V_m and V_L (which are assumed as indicators of the overall stability of the system). From this perspective, it should be recalled from Fig. 8 that both speeds are associated to the plunge instability. It is thus predictable that an adverse choice of parameters for the latter (as it is K_α=-1 from the worst-case analysis) is likely to worsen this scenario. The variable K_α represents hence a trade-off between two different objectives: on the one side further decreasing the LCO amplitude, and on the other preserving the airspeed range where LCO occurs. Built on these reflections, three different designs are considered, see Tab.2. In the table are expressed the suggested change of the variables as percentage from the nominal value. S_α is unaltered since it barely affects any of the instabilities and thus would represent an ineffective design change. K_h, I_α and I_β are modified according to the previous comments. The three designs differ only on the pitch stiffness K_α, in order to observe its global effect. The corresponding LCO amplitude curves are plotted in Fig. 11 against the original case.

Table 2 Change in the tailoring variables to achieve the LCO tailoring

	Design 1	Design 2	Design 3
K_α	0%	-20%	+20%
K_h	-20%	-20%	-20%
I_α	+20%	+20%	+20%
I_β	-20%	-20%	-20%
S_α	0%	0%	0%

All the proposed designs achieve the main goal of reducing the LCO amplitude as well as fulfilling the requirement of maintaining the same lowest LCO occurrence speed V_m, as shown by a comparison to the original curve. Design 2 reaches the minimum LCO amplitude among the curves but presents, as side effect, a drastic reduction in the value of V_L. This is in line with the previous analyses which suggested a reduction in K_α as beneficial to lower the LCO amplitude. They also pointed out that the same change would affect detrimentally the plunge stability, responsible for the linear flutter speed. Design 3 goes in the opposite direction for both objectives since it increases the value of this stiffness parameter. Finally Design 1, which does not alter the value of K_α, seems the best compromise since on one side it maintains the same linear flutter speed, and on the other it achieves a noticeable amplitude reduction. Of course other designs could be proposed which contemplate *absolute* variations of K_α smaller than 20% and thus span solutions between Design 1 and Design 3.

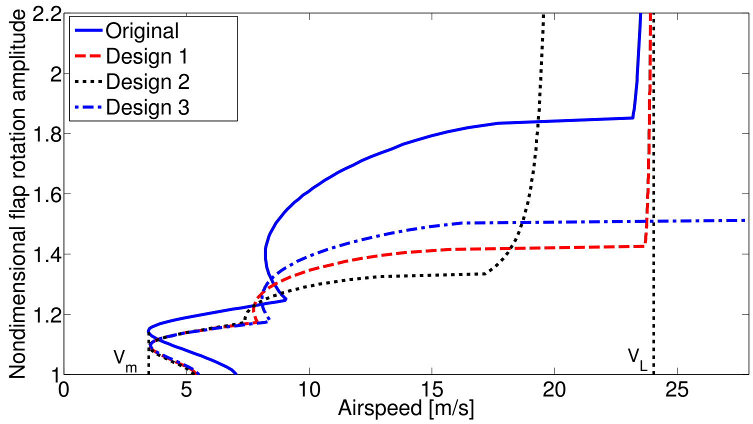

Fig. 11 Flap rotation LCO amplitudes $\frac{\beta_s}{\delta}$ after the values of the design variables are modified according to Tab.2 and comparison with the original graph

6 Conclusions

This work investigates a methodology to combine linear modeling of aeroelastic systems with Describing Function to take into account control surface freeplay and μ to perform quasi-linear analysis with uncertainties in the system. The contribution of the work is twofold.

The outcome of nominal analyses is presented, showing a good correlation with other benchmark results. The implications of using DF method as tool for nonlinear assessments are discussed. Moreover, it is stressed how DF is instrumental in guaranteeing the connection between the conditions of neutral stability evaluated in the quasi-linearized system and the conclusions inferred about the nonlinear response of the system in terms of onset, amplitude, frequency and stability of LCO.

The last section of the paper shows a possible application of μ analysis to actively or passively (depending on how the suggested methodology is implemented) modify the properties of the nonlinear response. In particular, μ is employed to understand which changes in the parameters values are more crucial to achieve a decrease of the LCO amplitude with the constraint to not affect the critical speeds of the system. The outlined procedure features a dual usage of this technique. It is first exploited its worst-case capability to identify the combination of parameters leading to the neutral stability condition (this, as explained, is equivalent to moving the LCO curve) with the smallest departure from the nominal values (optimal design changes). Secondly, a μ-based sensitivity is applied to establish which are, inside the variable space considered, the most effective and efficient parameters for the prescribed goal. The results in terms of proposed designs showcase the potential of the methodology.

Acknowledgements This work has received funding from the European Union's Horizon 2020 research and innovation programme under grant agreement No 636307, project FLEXOP.

References

1. R. J. Allemang and D. L. Brown. A correlation coefficient for modal vector analysis. *1st International Modal Analysis Conference*, 1982.
2. M.R. Anderson. Pilot-induced oscillations involving multiple nonlinearities. *J. of Guidance, Control and Dynamics*, Vol. 21(5):pp. 786–791, 1998.
3. D.H. Baldelli, R.C. Lind, and M. Brenner. Robust Aeroservoelastic Match-Point Solutions Using Describing Function Method. *Journal of Aircraft*, 42(6):1597–1605, 2005.
4. R. L. Bisplinghoff and H. Ashley. *Principles of Aeroelasticity*. Wiley, New York, 1962.
5. D Borglund. The μ-k method for robust flutter solutions. *Journal of Aircraft*, 41(5):1209–1216, 2004.
6. M.D. Conner, D.M. Tang, E.H. Dowell, and L.N. Virgin. Nonlinear Behavior of a Typical Airfoil Section with Control Surface Freeplay. A Numerical and Experimental Study. *Journal of Fluids and Structures*, 11(1):89 – 109, 1997.
7. B. Danowsky, P.M. Thompson, and S. Kukreja. Nonlinear Analysis of Aeroservoelastic Models with Free Play Using Describing Functions. *Journal of Aircraft*, 50(2):329–336, 2013.
8. E. Dowell, J. Edwards, and T. Strganac. Nonlinear aeroelasticity. *Journal of Aircraft*, Vol. 40(5), 2003.
9. A. Gelb and W. E. Vander Velde. *Multiple-Input Describing Functions and Nonlinear System Design*. McGraw-Hill, 1968.
10. J.T. Gordon, E.E. Meyer, and R.L. Minogue. Nonlinear Stability Analysis of Control Surface Flutter with Freeplay Effects. *Journal of Aircraft*, 45(6):1904–1916, 2008.
11. D. H Hodges and G A. Pierce. *Introduction to Structural Dynamics and Aeroelasticity; 2nd ed.* Cambridge Aerospace series. Cambridge University Press, New York, NY, 2011.
12. A. Iannelli, A. Marcos, and M. Lowenberg. Comparison of Aeroelastic Modeling and Robust Flutter Analysis of a Typical Section. IFAC ACA, August 2016.
13. A. Iannelli, A. Marcos, and M. Lowenberg. Modeling and Robust Body Freedom Flutter Analysis of Flexible Aircraft Configurations. IEEE MSC, September 2016.
14. M. Karpel. Design for Active and Passive Flutter Suppression and Gust alleviation. Technical Report 3482, NASA, 1981.
15. H. K. Khalil. *Nonlinear systems*. Prentice Hall, Upper Saddle River, (N.J.), 1996.
16. A. Kotikalpudi, H. Pfifer, and P. Seiler. Sensitivity of robust flutter boundary to model uncertainties in aeroservoelastic systems. AIAA Scitech, January 2016.
17. R. Lind and M. Brenner. *Robust Aeroservoelastic Stability Analysis*. Advances in Industrial Control. Springer London, 2012.
18. Liu, L. and Dowell, E. H. Harmonic Balance Approach for an Airfoil with a Freeplay Control Surface. *AIAA Journal*, 43(4):802–815, April 2005.
19. A. Packard and J. Doyle. The Complex Structured Singular Value. *Automatica*, 29(1), 1993.
20. D.M. Pitt and P. Bansal. Uncertainties in control surface free-play and structural properties and their effect on flutter and LCO. AIAA Scitech Conference, January 2014.
21. H. Shukla and M. Patil. Control of Limit Cycle Oscillation Amplitudes in Nonlinear Aerelastic Systems using Nonlinear Normal Modes. AIAA Scitech Conference, January 2016.
22. D. Tang, E.H. Dowell, and L.N. Virgin. Limit Cycle Behavior of an Airfoil with a Control Surface. *Journal of Fluids and Structures*, 12(7):839 – 858, 1998.
23. T. Theodorsen. General Theory of Aerodynamic Instability and the Mechanism of flutter. Technical Report 496, Naca, 1935.
24. P. Wiggins. *Introduction to Applied Nonlinear Dynamical Systems and Chaos*. Springer-Verlag New York, 2003.
25. K. Zhou, J. C. Doyle, and K. Glover. *Robust and Optimal Control*. Prentice-Hall, Inc., Upper Saddle River, NJ, USA, 1996.